5-7-2004

Photo-Responsive and Electrically Switchable Mesophases in a Novel Class of Achiral Bent-Core Azo Compounds

Veena Prasad

Shin-Woong Kang
Kent State University - Kent Campus

Xianghong Qi
Kent State University - Kent Campus

Satyendra Kumar
Kent State University - Kent Campus, skumar@kent.edu

ARTICLE

Journal of Materials Chemistry
www.rsc.org/materials

Photo-responsive and electrically switchable mesophases in a novel class of achiral bent-core azo compounds†

Veena Prasad,[a] Shin-Woong Kang,[b] Xianghong Qi[b] and Satyendra Kumar*[b]

[a]*Center for Liquid Crystal Research, P.B.No.1329. E-mail: Jalahalli, Bangalore – 560013, India*
[b]*Department of Physics, Kent State University, Kent OH 44242, USA. E-mail: satyen@xray.kent.edu*

Received 11th November 2003, Accepted 25th February 2004
First published as an Advance Article on the web 17th March 2004

The first examples of electrically switchable and photo-responsive mesophases in a novel class of bent-core azo compounds, consisting of only five aromatic rings and no imino functionality (–CH=N–), are reported. The mesophases have been identified as B_1, B_2 and a new mesophase, B_x, on the basis of the results of polarizing optical microscopy, differential scanning calorimetry, X-ray diffraction, and electro-optical response. Preliminary but profound photo-induced effects on the transition temperature from isotropic to the B_2 mesophase of one of the azo compounds are also presented.

I. Introduction

Achiral bent-core mesogens[1] are new and an exciting area of research in the field of ferro-/antiferro-electric liquid crystals.[2–6] Although the constituent molecules here are achiral, some of the phases exhibited by such compounds are often found to be chiral and show interesting electro-optical properties with potential for use in practical applications.[5] Recently, we have taken a novel approach[7] to synthesize bent-core compounds by introducing an azo (–N=N–) linkage in these molecules. The introduction of an azo functionality adds in a new dimension, namely photochromism, to this field as the linkage –N=N– undergoes *trans–cis* isomerisation in the presence of UV light. Thus, the physical properties of such bent-core compounds become multifold and can be exploited for technological applications.

The observation of photosensitivity and electrical switching at fairly low temperatures in the mesophases of a series of these bent-core azo compounds[8] encouraged us to go one step further, *i.e.*, synthesize a second series of bent-core azo compounds[9] with slight modifications in the previously reported azo molecules.[8] Here, we report results of our preliminary investigations to characterize the mesophases and to understand the photo-induced effects in the antiferroelectric B_2 mesophase of one of the azo compounds.

For accurate and convenient measurements of physical properties and phase identification, it is important to have compounds that are thermally stable and resistant to moisture and light. In addition, they should exhibit mesophases enantiotropically, at reasonably low temperatures and for a reasonably wide temperature range. Although, our previous bent-core azo compounds[8,9] were found to be thermally very stable and exhibit enantiotropic mesomorphism at low temperatures, they contained an imino functionality in the molecule. Generally, the compounds with an imino functionality have limited thermal, hydrolytic, and photochemical stability.[10] To overcome this problem, we synthesized a new series of bent-core azo compounds **1a–e** and **2a–e** whose molecular structures are shown in Fig. 1. These compounds exhibit mesomorphism at relatively low temperatures (77–123 °C) for fairly wide temperature ranges (3–30 K). The mesophases are found to super cool considerably. This paper describes the synthesis and mesophase characterization of compounds **1a–e** and **2a–e**. A study of their electro-optical behavior and the photo-induced effects on the transition temperature from the isotropic to the B_2 mesophase of compound **2e** is also reported.

II. Experimental details

II.1. Synthesis

AR quality chemicals and solvents were obtained locally and the solvents were dried using the standard procedures as and when required. The purity and the chemical structures of all the compounds synthesized were confirmed by the spectral data. IR spectra were recorded using a Perkin-Elmer 1000 spectrometer. ^{1}H NMR spectra were recorded in $CDCl_3$ on a 200 MHz Bruker Aveance Series DPX-200 NMR spectrometer, using Me_4Si as an internal standard. Microanalyses were performed using a Eurovector Elemental Analyzer, Model Euro EA 3000.

All the homologues of the two series **1a–e** and **2a–e** are synthesized following the scheme shown in Fig. 2. Thus, the aldehyde **4**, obtained in three steps, starting from 4-n-dodecyloxybenzoic acid and 4-hydroxybenzaldehyde, was subjected to oxidation using Jones reagent[11] to get the key intermediate, acid **3**. This acid **3** was then esterified with 4-n-alkyl/alkyloxy-4′-hydroxyazobenzenes in the presence of 1,3-dicyclohexylcarbodiimide (DCC) and dimethylaminopyridine (DMAP) as catalyst using dry dichloromethane as solvent. The final bent-core compounds **1a–e** and **2a–e** thus obtained were first purified by column chromatography and then by a minimum of two recrystallisations using butan-2-one as solvent.

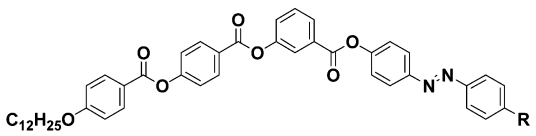

1a-e: R = OC_4H_9, OC_6H_{13}, OC_8H_{17}, $OC_{10}H_{21}$, $OC_{12}H_{25}$

2a-e: R = C_4H_9, C_6H_{13}, C_8H_{17}, $C_{10}H_{21}$, $C_{12}H_{25}$

Fig. 1 Molecular structures of the azo compounds of the two series **2a–e** and **1a–e**.

† Electronic supplementary information (ESI) available: colour versions of Figs. 3, 4, 7 and 8. See http://www.rsc.org/suppdata/jm/b3/b314482h/

DOI: 10.1039/b314482h

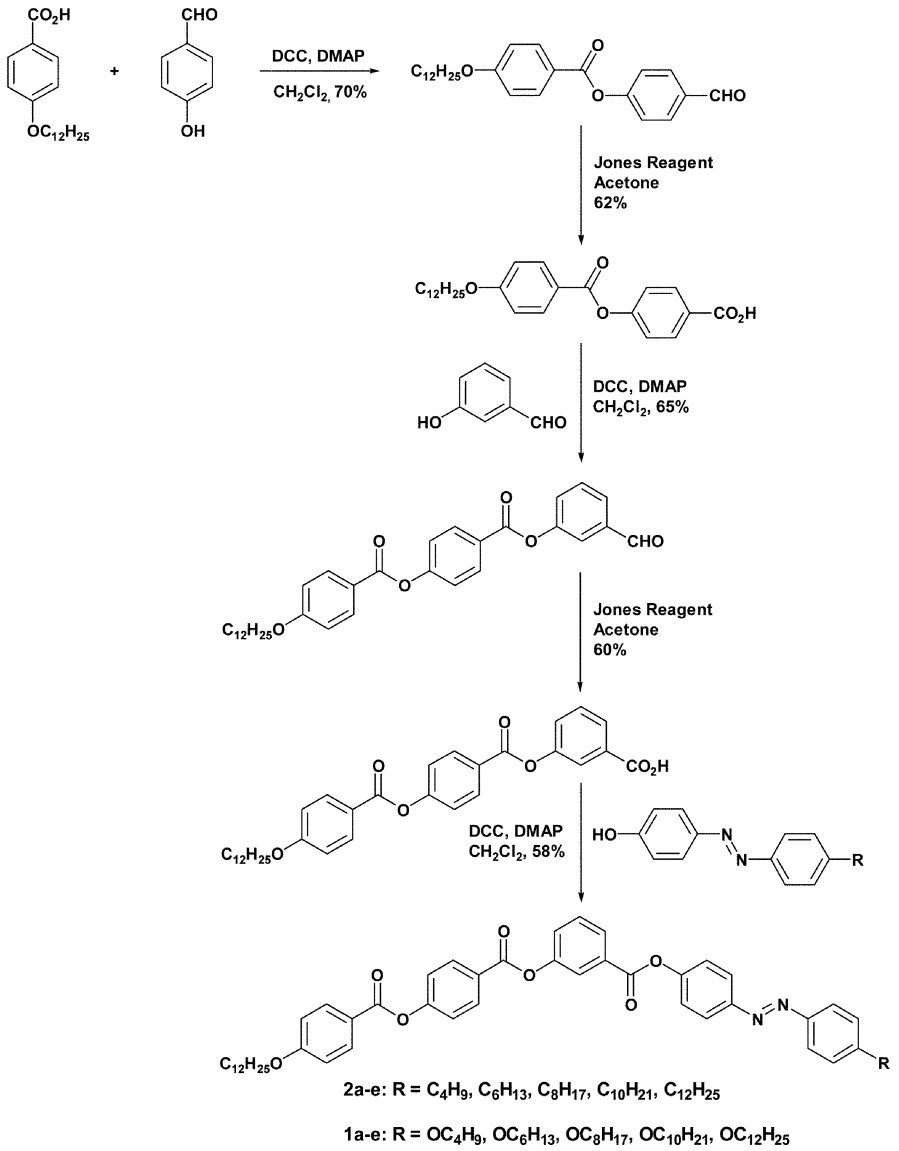

Fig. 2 Synthesis scheme followed for the synthesis of **1a–e** and **2a–e**.

The spectral data and the microanalyses obtained for all the compounds were in agreement with their chemical structures. The analytical data obtained for the intermediate compounds **4** and **3** and for one representative final compound, **2e**, are given below.

Compound 4: ^{1}H NMR (200 MHz, $CDCl_3$) δ: 10.02 (s, 1H, –CHO), 6.9–8.16 (m, 12H, ArH), 4.05 (t, 2H, Ar–OCH_2), 1.27–1.86 (m, 20H, –CH_2–), 0.88 (t, 3H, –CH_3). Elemental anal.: calcd for $C_{33}H_{38}O_6$, C, 74.69, H, 7.22; found, C, 74.62, H, 7.21%.

Compound 3: ^{1}H NMR (200 MHz, $CDCl_3$) δ: 6.97–8.31 (m, 12H, ArH), 4.05 (t, 2H, Ar–OCH_2), 1.27–1.86 (m, 20H, –CH_2), 0.88 (t, 3H, –CH_3). Elemental anal.: calcd for $C_{33}H_{38}O_7$, C, 72.51, H, 7.01; found, C, 72.48, H, 7.06%.

Compound 2e: IR ν_{max}/cm^{-1} (KBr pellet): 2916, 2850, 1732, 1605, 1469, 1282. ^{1}H NMR (200 MHz, $CDCl_3$) δ: 6.96–8.32 (m, 20H, ArH), 4.05 (t, 2H, Ar–OCH_2), 2.68 (t, 2H, Ar–CH_2), 1.26 – 2.72 (m, 40H, –CH_2–), 0.88 (m, 6H, –CH_3). Elemental anal.: calcd for $C_{57}H_{70}N_2O_7$, C, 76.48, H, 7.88, N, 3.13; found, C, 76.56, H, 7.98, N, 3.13%.

II.2. Mesophase characterization

The microscopic textural observations were carried out using a Mettler FP82HT hot stage in conjunction with a Leitz DMRXP polarizing microscope. The brightness of microscope lamp was adjusted to different levels and temperature lowered to determine the effect of illumination on transition temperatures. The enthalpies associated with different transitions and the transition temperatures were also determined using differential scanning calorimetry (DSC7, Perkin-Elmer). The heating and cooling rates were 5 °C min^{-1}. To test the sensitivity of the transitions to light, DSC scans were conducted without placing the lid on the sample cell to permit measurements with and without illumination of the sample with white light.

For structural characterization, the samples were sealed in 1 mm diameter Lindeman capillaries with 10 μm thick walls. The samples were taken above the clearing point and cooled in the presence of a magnetic field of $\sim$2.5 kG from the isotropic phase to the first liquid crystalline phase. This procedure sometimes results in well aligned domains. X-Ray studies were performed at the Advanced Photon Source of Argonne National Laboratory using the Midwestern Universities Collaborative Team's spectrometer on Sector 6. An X-ray wavelength of 1.26515 Å was used. The diffraction patterns were collected using a high-resolution MAR3450 area detector placed at a distance of 362.9 mm from the sample. The data were calibrated against a powdered silicon standard. Sample temperature was controllable with a precision of $\pm$0.1 °C using a home made oven and temperature controller. The 2θ scans were generated from the 2-D diffraction patterns using the

software package FIT2D developed by A. P. Hammersley of the European Synchrotron Radiation Facility.

The UV-vis absorption spectra were obtained at room temperature using a HP8453 UV-vis spectrometer for a fresh sample of **2e** dissolved in hexane (or dichloromethane, 4×10^{-5} mol L^{-1}) and after its prolonged exposure to 365 nm light. This exposed sample was placed in the dark and the absorption spectrum measured every two hours to determine the extent of change in *cis–trans* population.

For the electro-optical studies, the sample was sealed in flat glass cells of $\sim$1.8 μm thickness. Glass plates with a transparent but electrically conducting indium-tin-oxide (ITO) layer and polyimide alignment layers with low ($\sim 1^{\circ}$) pretilt angle were assembled with antiparallel rubbing directions. The electro-optical response was studied using square waveforms of the applied voltage. The spontaneous polarization, ***P***, was measured using a triangular waveform of 100 Hz and a peak voltage, V_p, ranging from 0 to 80 V with no light exposure. The applied signal and current through the sample were recorded using a Tektronix oscilloscope model TDS-340A. During these measurements, only minimal brightness of light was used for short periods of time to record the optical textures. The effect of light exposure on the phase behavior was determined by observing the textural changes while cooling from the isotropic phase under different degrees of illumination.

III. Results and discussion

III.1. Phase behavior

In our present study, we have synthesized ten new bent-core azo compounds shown in Fig. 1 belonging to two different homologous series **1a–e** and **2a–e**. All of the compounds exhibit liquid crystalline phases. The thermal behavior of all these compounds was studied by polarizing optical microscopy and differential scanning calorimetry. The transition temperatures (°C) and the associated enthalpies (kJ mol^{-1}) obtained from DSC thermograms are given in Table 1. All compounds are thermally very stable as confirmed by the reproducibility of thermograms on several heating and cooling cycles. Several of the compounds show crystal to crystal transitions before melting. In some cases, the solvent crystallized and melt crystallized solids show different melting points. This may be due to different crystal forms obtained during the two different processes.[12]

We fixed the chain length at one end of the molecule to be $OC_{12}H_{25}$. The chain length R at the other end of the molecule was systematically varied, as in our previous study.[8] R was chosen to be either an alkyloxy (**1a–e**) or an alkyl (**2a–e**) chain. In the case of series **1a–e**, except for the lowest homologue **1a** with R = OC_4H_9, all other higher homologues are found to be enantiotropic in nature. Compounds **1a** and **1b** (R = OC_6H_{13}) show the B_1 mesophase whereas compound **1c** (R = OC_8H_{17}) shows two different mesophases. It exhibits a monotropic unidentified B_x phase in addition to the enantiotropic B_1 mesophase. Compounds **1d** (R = $OC_{10}H_{21}$) and **1e** (R = $OC_{12}H_{25}$) exhibit the enantiotropic B_2 phase. In the series **2a–e**, all compounds except the highest homologue **2e** with R = $C_{12}H_{25}$, exhibit only a monotropic mesophase. Compound **2e** is enantiotropic, exhibiting the B_2 mesophase. Compound **2d** with R = $C_{10}H_{21}$, exhibits the monotropic B_2 mesophase. The remaining lower homologues show only the monotropic B_1 phase. It is evident from Table 1 that the mesophases of the alkyl substituted compounds, **2a–e**, supercool more than the mesophases of the alkyloxy compounds, **1a–e**, before crystallization.

For a complete characterization and determination of the phase structure, electro-optical behavior, and photo-sensitivity we selected three representative compounds, **1c**, **1e**, and **2e** for further investigations.

Compound **1c**, on cooling from the isotropic phase, forms a fan-shaped texture along with a mosaic pattern in some regions. This characteristic texture of the B_1 phase is shown in Fig. 3(a). On further cooling, the B_1 phase transforms in to an unknown B_x phase, Fig. 3(b). The appearance of striations over the texture of the B_1 phase upon cooling to the B_x phase is similar to the changes seen in the texture at the transition upon cooling from the Crystal B to the Crystal E phase[13] in calamitic liquid crystals where it is indicative of the freezing of rotational diffusional motion about the molecules' long axis. This behavior is absent in the other two compounds, **1e** and **2e**, studied. On cooling from the isotropic phase, these compounds form textures that are characteristic of the B_2 phase, shown in Fig. 3(c) and (d), respectively.

III.2. Structure of phases

The results of X-ray investigations of the two phases of compound **1c** are shown in Fig. 4. The sample melts into the B_1 phase that exhibits a liquid like diffraction ring at large angle (4.57 Å) and two rings at length scales of 36.4 $\pm$ 0.2 Å and 23.6 $\pm$ 0.1 Å, which is typically observed in the B_1 phase. When the sample is cooled slowly from the isotropic phase in the presence of a weak magnetic field, it appears to align well, as clear from Fig. 4(a). This diffraction pattern has its origin in a two dimensional rectangular cell with dimensions of 36.4 $\pm$ 0.2 and 30.4 $\pm$ 0.2 Å, and is very similar to the previously reported results for the phase B_1 by Pelzl *et al.*[5] The peaks (see Fig. 5) obtained in the B_1 phase are found to be sharper upon cooling from the isotropic phase due to improved alignment.

Upon further cooling the sample **1c** below 111 °C, the system undergoes a transition to the phase we call the B_x phase. The enthalpy of transition is small (0.15 kJ mol^{-1}) leading us to conclude that this is either a second order or weakly first order transition. The B_x phase has a very interesting diffraction pattern which is shown in Fig. 4(b). The X-ray scattering intensity as a function of scattering angle is shown in Fig. 5 for sample **1c** in the different phases. The first small angle reflection corresponds to 54.2 $\pm$ 1 Å. Up to 9 harmonics of this primary reflection corresponding to lattice dimensions of 54.2/*n*, where

Table 1 Phase transition temperatures (°C) obtained from the DSC thermograms and enthalpies (kJ mol^{-1}) of transitions given in parentheses for the azo compounds **1a–e** and **2a–e**

Compound	R	1st Heating	1st Cooling
1a	OC_4H_9	**Cr** 121.5 (73.4) **I**	**I** 120.0 (13.9) $\mathbf{B_1}$ 110.0 (44.3) **Cr**
1b	OC_6H_{13}	**Cr** 116.4 (57.8) $\mathbf{B_1}$ 122.0 (15.8) **I**	**I** 120.9 (15.5) $\mathbf{B_1}$ 101.7 (43.0) **Cr**
1c	OC_8H_{17}	**Cr** 116.5 (63.4) $\mathbf{B_1}$ 120.4 (18.1) **I**	**I** 119.4 (15.2) $\mathbf{B_1}$ 110.5 (0.15) $\mathbf{B_x}$ 98.8 (37.6) **Cr**
1d	$OC_{10}H_{21}$	**Cr** 117.5 (74.1) $\mathbf{B_2}$ 120.8 (16.8) **I**	**I** 119.8 (17.2) $\mathbf{B_2}$ 104.5 (70.1) **Cr**
1e	$OC_{12}H_{25}$	**Cr** 117.8 (71.9) $\mathbf{B_2}$ 122.9 (17.7) **I**	**I** 121.5 (17.6) $\mathbf{B_2}$ 102.7 (74.2) **Cr**
2a	C_4H_9	**Cr** 126.4 (67.9) **I**	**I** 101.5 (11.2) $\mathbf{B_1}$ 98.2 (28.5) **Cr**
2b	C_6H_{13}	**Cr** 121.5 (62.6) **I**	**I** 108.0 (12.5) $\mathbf{B_1}$ 92.5 (25.3) **Cr**
2c	C_8H_{17}	**Cr** 117.3 (52.2) **I**	**I** 109.3 (11.5) $\mathbf{B_1}$ 86.8 (23.5) **Cr**
2d	$C_{10}H_{21}$	**Cr** 115.8 (56.5) **I**	**I** 114.7 (13.7) $\mathbf{B_2}$ 84.3 (27.8) **Cr**
2e	$C_{12}H_{25}$	**Cr** 110.5 (40.4) $\mathbf{B_2}$ 115.5 (15.1) **I**	**I** 114.5 (14.9) $\mathbf{B_2}$ 77.4 (32.1) **Cr**

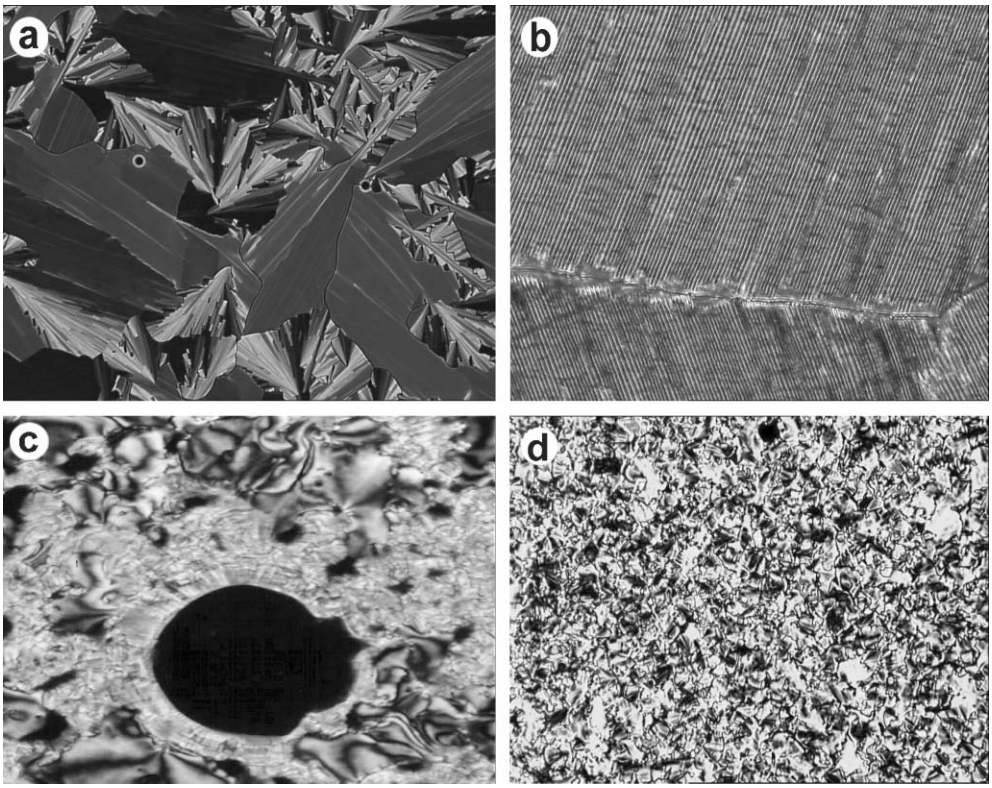

Fig. 3 (a) The texture of B_1 phase at 119.0 °C, obtained on cooling the isotropic phase of compound **1c**. On further cooling we obtain the phase B_x shown in (b). Observe the striped pattern, shown magnified (400 ×), formed on the fan-shaped texture of the B_1 phase. (c) The unspecified texture of the B_2 phase (along with the schlieren texture in some regions) exhibited by compound **1e** at 114.5 °C and (d) the schlieren texture of the B_2 phase of **2e**.

$n = 1, 2, ...9$, are observed with great ease. Several reflections are observed in the range from 4.79 to 3.22 Å from the crystalline in-plane order. The presence of such a large number of harmonics of the small angle peak points to highly well defined layers stacked with nearly single crystal quality. However, this phase does not have true three-dimensional order as evident from the absence of any intervening reflections, *i.e.*, between the peaks corresponding to the in-plane structure and small angle peaks arising from smectic layers. Based on these data, we conclude that this phase consists of

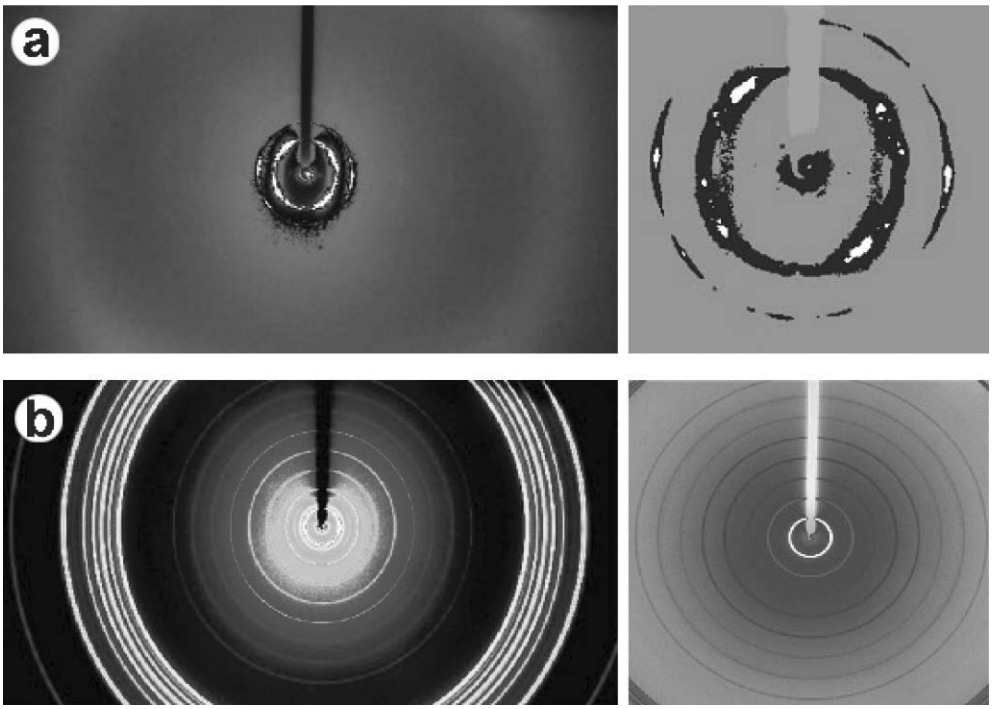

Fig. 4 X-Ray diffraction patterns of sample **1c** in different phases. The panels at right show the small angle scattering at higher magnification. (a) B_1 phase of sample at 115 °C. The sample is partially aligned and the small angle pattern resembles the typical pattern of the B_1 phase. (b) In the B_x phase at (109 °C) ~1.5 K below the transition, two sets of rings, 9 harmonics of the reflection at 54.2 Å are seen at small angles and the second set at large angles.

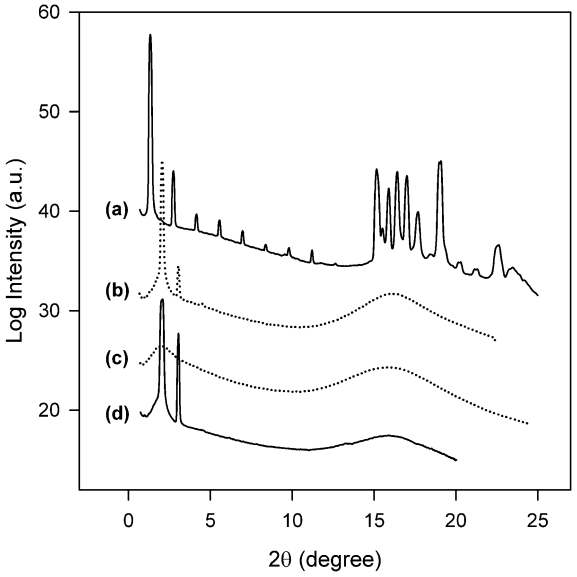

Fig. 5 Intensity *vs.* diffraction angle 2θ for sample **1c** in different phases, for X-ray wavelength of 1.26515 Å. (a) In the B_x phase at 109 °C, 9 harmonics of the reflection at 54.2 ± 1 Å are visible, (b) in the B_1 phase at 115 °C, (c) isotropic phase at 129 °C, and (d) in the B_1 phase after cooling from the isotropic phase, at 115 °C.

extremely well defined bilayers with crystalline in-plane order but no interplanar correlations of the in-plane structure from one layer to another. One expects the layers in such a phase to be able to freely slide relative to each other and act like a highly lubricating medium. This expectation was qualitatively confirmed by shearing the phase between two glass plates. To the best of our knowledge, such a phase has not been previously reported in bent-core materials.

The X-ray diffraction patterns of compounds **1e** and **2e** were taken at 120 and 98 °C, respectively, after cooling from the isotropic phase. The sample is partially aligned by the magnetic field and was evident from the intensity distribution of the inner rings. Fig. 6 shows the X-ray intensity as a function of diffraction angle for the three samples in their respective B_1 or B_2 phases. For sample **1e**, small angle peaks appear at 41.7 ± 0.8 Å, 20.42 ± 0.1 Å, and 13.51 ± 0.05 Å while the large angle diffuse peak appears at 4.57 Å. For sample **2e**, the small angle condensed reflections correspond to 42.8 ± 0.8 Å, 21.06 ± 0.1 Å, and 13.95 ± 0.05 Å, and the large angle diffuse peak at 4.70 Å. For this sample, no magnetic field alignment is observed. For both samples, the first peak is the brightest and the ratio of the lattice spacings corresponding to the three reflections is 1:2:3 indicating a lamellae or smectic type ordering.

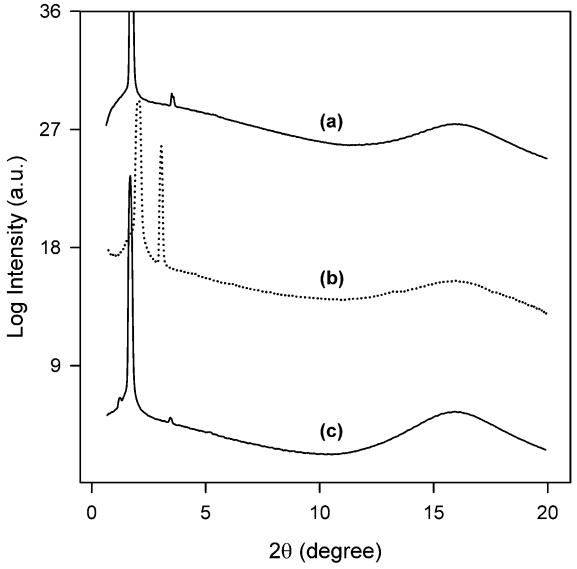

Fig. 6 Intensity *vs.* diffraction angle 2θ for the three samples studied: (a) **1e** at 120 °C, (b) **1c** at 115 °C, and (c) **2e** at 98 °C. The X-ray wavelength used was 1.25616 Å. The curves have been shifted vertically for clarity. The third harmonics for samples **1e** and **2e** are not visible on this scale.

III.3. Electro-optical properties

Phase B_1 of sample **1c** does not exhibit any response to an applied electric field, as one would expect. However, the B_2 phases of samples **1e** and **2e** respond to an applied field in an antiferroelectric manner which can be visually observed *via* the changes in their optical textures. These textural change occur when a field of $\sim \pm 20$ V μm^{-1} is applied perpendicularly to the cell, see Figs. 7 and 8 for samples **1e** and **2e**, respectively. Fig. 9 shows the current flow through cells filled with compounds **1e** and **2e**, in response to an applied triangular wave electric field of amplitude reaching ± 40 V μm^{-1}. The fact that these materials switch in an antiferroelectric manner is confirmed by

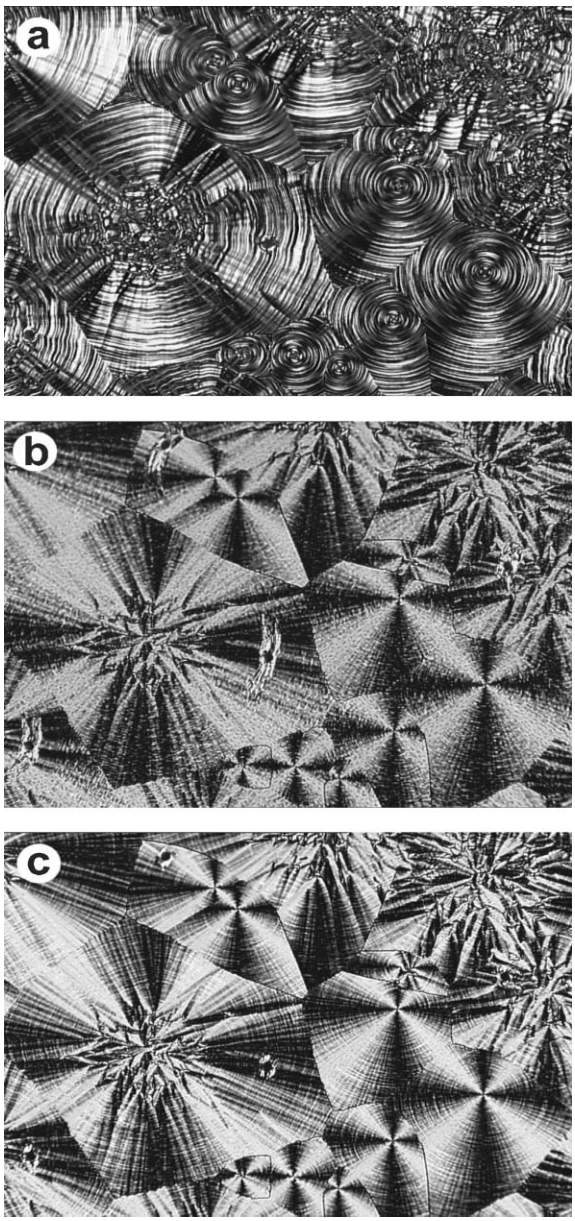

Fig. 7 Optical textures of sample **1e** (a) with +20 V μm^{-1}, (b) no field, and (c) with −20 V μm^{-1}. Polarizer/analyzer is parallel/perpendicular to the image frame.

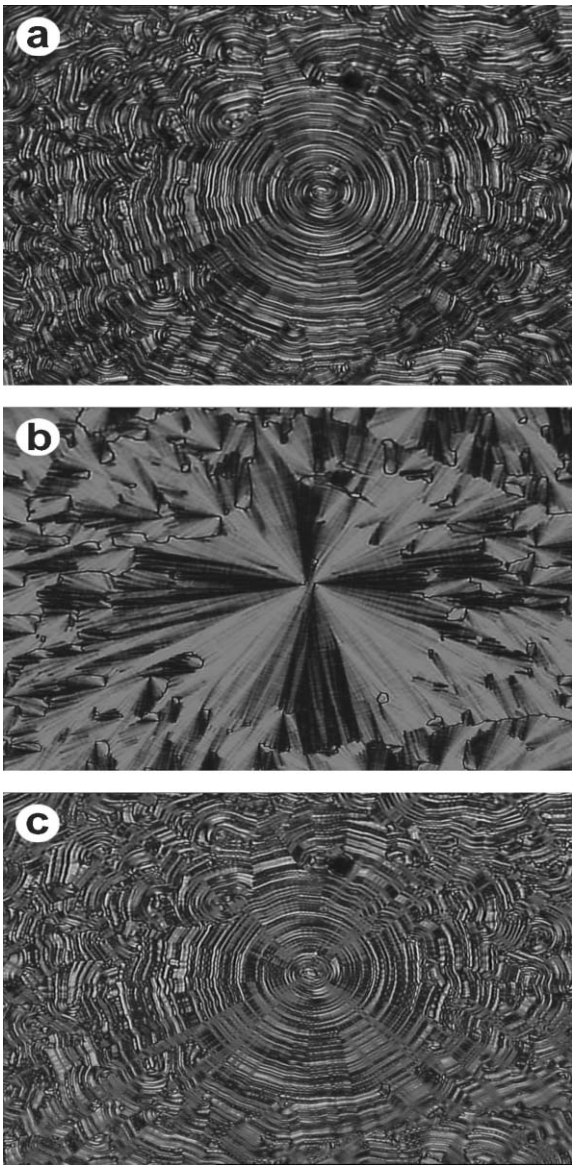

Fig. 8 Optical textures of sample **2e** (a) with an applied field of $+20$ V μm^{-1}, (b) without field (c) with -20 V μm^{-1}. Polarizer/analyzer is parallel/perpendicular to the image frame.

the presence of two polarization reversal peaks. From the measurements, we calculate the spontaneous polarizations, ***P***, to be 419 nC cm^{-2} at 120 °C for **1e** and 276 nC cm^{-2} at 110 °C for **2e**. Based on these results we conclude that the B_2 phase exhibited by these materials is the anticlinic antiferroelectric, or the SmC_AP_A[6,8,14,15] phase.

III.4. Photo-sensitivity

The textures of these materials are found to change when the brightness of the microscope lamp was varied, indicating sensitivity to light. Upon performing UV-vis absorption spectroscopy on compound **2e**, light radiation in the wavelength range 290–380 nm is found to be strongly absorbed with the maximum at 335 nm. This can be attributed to the π–π* transition of the chromophore in the molecule.[16] After prolonged exposure to 365 nm light which falls within this absorption band, the absorption at 440 nm appears to increase while dropping in the band at 335 nm. This suggests that the sample freshly prepared in the dark is composed predominantly of *trans* conformation in which the molecules absorb 335 nm and transform to the *cis* state. The molecules in the *cis* form absorb light in the 400–480 nm range centered at 440 nm

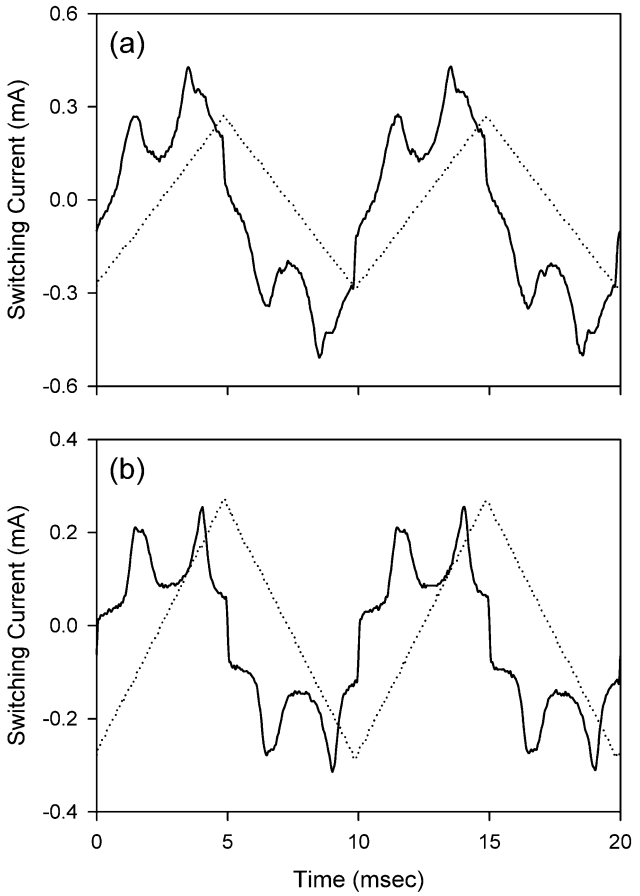

Fig. 9 Electro-optical response of sample (a) **1e** at 120 °C and (b) **2e** at 110.0 °C to an applied triangular waveform of frequency 100 Hz and fields of 40 V μm^{-1}.

corresponding to the n–π* transition,[17,18] and consequently transform to the *trans* conformation. However, when kept in the dark at room temperature after exposure to 365 nm light, its return to *trans* state appears to be very slow. The UV-vis absorption spectra of the sample as (a) freshly prepared, (b) exposed to 365 nm light, and (c) after keeping the exposed sample in the dark for 20 hours are shown in Fig. 10. All three compounds show similar behavior of *trans–cis* isomerization upon UV-illumination but the absorption efficiency at ~335 nm and subsequent increase in absorption for wavelengths near 440 nm is found to be highest for sample **2e** followed by **1e** and then **1c**.

In order to determine the effect of light exposure on the isotropic to the B_2 phase transition, sample **2e** contained in an electro-optical cell is cooled in a Mettler hot stage from the isotropic phase to the B_2 phase, under different degrees of illumination. The temperature at which the characteristic texture of the B_2 phase appears is recorded. The microscope lamp has both 350 and 440 nm wavelengths, see inset in Fig. 11, at the powers used. The intensity of 350 nm is higher than 440 nm at all power levels and with increasing intensity, the system becomes increasingly populated with *cis* isomers. The transition temperature drops by more than 4 K as the total incident power is increased from 0 to ~0.85 mW cm^{-2}. The biggest change in transition temperature was obtained in sample **2e** followed by **1e** and **1c**, which can be corroborated by the efficiency of peak reduction in the wavelength band at 335 nm described above. This decrease is similar in nature to that observed when the sample decomposes or when impurities are added. The presence of *cis* isomers appears to act as an impurity in reducing the transition temperature as previously observed in azo-dye doped rod-like azo LCs.[17,18] In this case,

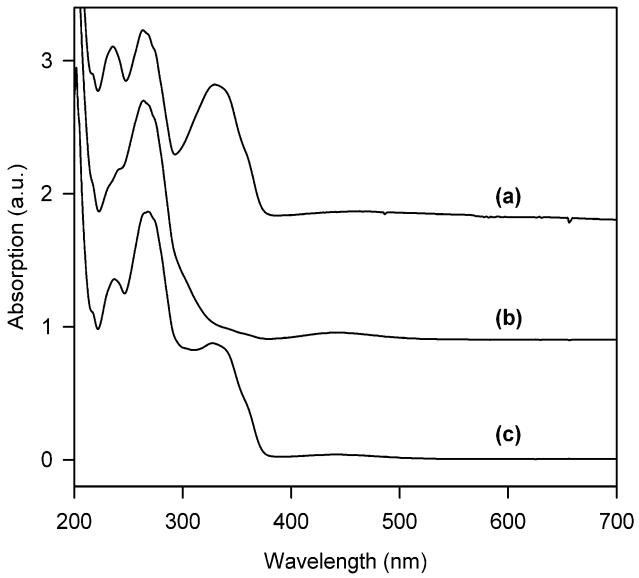

Fig. 10 UV-vis absorption spectra of sample **2e** (a) fresh sample, (b) after exposure to 365 nm light the absorption peak in the band 290–380 nm disappears while absorption from 400–480 nm increases, and (c) after keeping the exposed sample in total darkness for 20 h the absorption band at 335 nm reappears.

cis isomers may intervene in the molecular interaction (or packing) between *trans* isomers, which result in banana mesophases.

To further test how this change in *trans–cis* isomer ratio affects the phase behavior, we conducted DSC studies on sample **2e** without the sample cell cover so that scans could be conducted with white light illumination; the results for sample **2e** are shown in Fig. 12. The isotropic to B_2 and B_2 to crystal phase transition temperatures are lowered by more than 0.5 and 1 K, respectively. The change in enthalpy at these two transitions is also found to decrease by $\geqslant 0.5$ J g^{-1}. The DSC scans performed with no illumination on a fresh sample can be reproduced after the sample is allowed to crystallize, suggesting

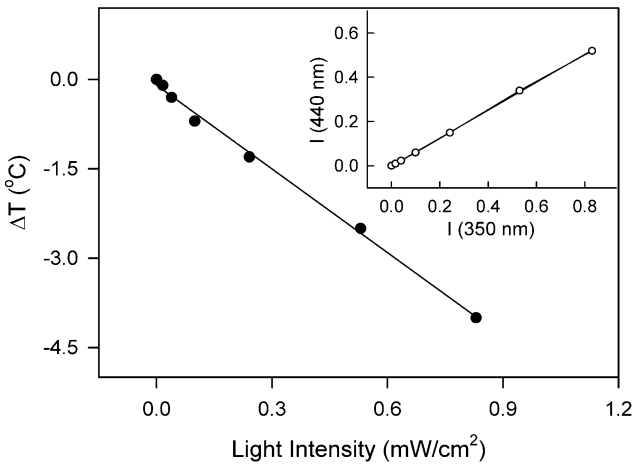

Fig. 11 Change in the transition temperature from the isotropic to the B_2 phase of compound **2e** as a function of incident power per unit area at 350 nm. The inset shows the relative intensity of the 350 and 440 nm lines in the microscope lamp's spectrum.

that the observed differences in transition temperatures and transition enthalpies are due to conformational changes and not the sample decomposition.

In order to further verify that sample decomposition is not responsible for the observed changes, thin layer chromatography (TLC) tests were performed on a freshly prepared solution in $CHCl_3$, and after exposure to ambient light for 4–5 hours. The fresh sample TLC results in one spot while the exposed sample yields two spots. The exposed solution is then allowed to evaporate and crystallize. When this dried sample is re-dissolved in $CHCl_3$ and TLC conducted under darkness, only one spot is obtained. These observations show that the molecules are transforming to the *cis* conformation in solution under ambient illumination and back to the *trans* state when the solvent is removed. These observations show that the effects of illumination are reversible and are not associated with sample decomposition with time or due to illumination.

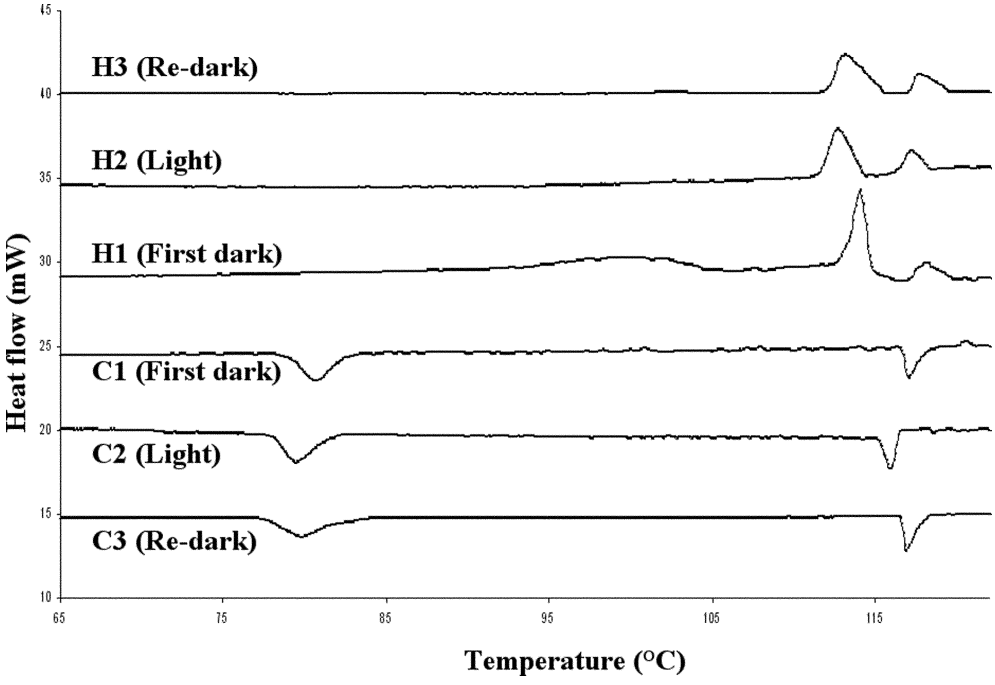

Fig. 12 DSC thermograms, H1 and C1, of fresh compound **2e** taken in total darkness upon first heating and cooling, respectively in the dark. Curves H2 and C2 represent the heating and cooling scans, respectively, under illumination with white light. The isotropic to B_2 phase transition temperature is lowered and transition enthalpy reduced. Curves H3 and C3 were obtained with no illumination after permitting the sample to crystallize.

IV. Summary

In conclusion, we have reported the synthesis and phase behavior of photosensitive unsymmetric bent-core azo compounds containing five aromatic rings and no imino linkages. The measurements performed on three compounds reveal the nature and structure of their liquid crystalline phases, which are found to be the anticlinic–antiferroelectric SmC_AP_A (or antiferroelectric B_2) in compounds **1e** and **2e** and the B_1, and the new B_x phases for sample **1c**. The B_x phase appears to be made of nearly crystalline planes with no structural correlations between smectic layers. These photochromic and antiferroelectrically responsive materials should find use in novel electro-optical and photonic applications. Detailed and quantitative investigations on their photosensitivity and electro-optical properties are presently in progress.

Acknowledgements

This research was supported in part by the US National Science Foundation grant DMR-0312792. The use of the Advanced Photon Source (APS) was supported by the US Department of Energy, Basic Energy Sciences, Office of Science, under Contract No. W-31-109-Eng-38. The Midwest Universities Collaborative Access Team (MUCAT) sector at the APS is supported by the US Department of Energy, Basic Energy Sciences, Office of Science, through the Ames Laboratory under Contract No. W-7405-Eng-82. The authors thank Professor S. Ramakrishnan of the Indian Institute of Science for very helpful discussions.

References

1 T. Niori, T. Sekine, J. Watanabe, T. Furukava and H. Takezoe, *J. Mater. Chem.*, 1996, **6**, 1231; J. Watanabe, T. Niori, T. Sekine and H. Takezoe, *Jpn. J. Appl. Phys.*, 1998, **37**, L139.

2 D. Shen, S. Diele, G. Pelzl, I. Wirth and C. Tschierske, *J. Mater. Chem.*, 1999, **9**, 661.

3 G. Pelzl, S. Diele, A. Jákli, C. H. Lischka, I. Wirth and W. Weissflog, *Liq. Cryst.*, 1999, **26**, 135.

4 D. Shen, A. Pegenau, S. Diele, I. Wirth and C. Tschierske, *J. Am. Chem., Soc.*, 2000, **122**, 1593.

5 G. Pelzl, S. Diele and W. Weissflog, *Adv. Mater.*, 1999, **11**, 707 and references therein.

6 D. M. Walba, E. Korblova, R. Shao, J. E. Maclennan, D. R. Link, M. A. Glaser and N. A. Clark, *Science*, 2000, **288**, 2181.

7 V. Prasad, D. S. S. Rao and S. K. Prasad, *Liq. Cryst.*, 2001, **28**, 643; V. Prasad, *Mol. Cryst. Liq. Cryst.*, 2001, **363**, 167.

8 V. Prasad, S-W. Kang and S. Kumar, *J. Mater. Chem.*, 2003, **13**, 1259.

9 V. Prasad and A. Jákli, *Presented at the 9th International Conference on Ferroelectric Liquid Crystals*, Dublin, Ireland, 2003, August 24–29 (Poster No. P-59).

10 D. Shen, S. Diele, I. Wirth and C. Tschierske, *Chem. Commun.*, 1998, 2573.

11 M. Lai, L. Liu and H. Liu, *J. Am. Chem. Soc.*, 1991, **113**, 7388.

12 M. E. Neubert, in *Liquid Crystals: Experimental Study of Physical Properties and Phase Transitions*, ed. S. Kumar, Cambridge University Press, London, 2001, ch. 3.

13 D. Demus and L. Richter, *Textures of Liquid Crystals*, Verlag Chemie, New York, (1978.

14 D. R. Link, G. Natale, R. Shao, J. E. Maclennan, E. Korblova and D. M. Walba, *Science*, 1997, **278**, 1924.

15 D. A. Coleman, J. Fernsler, N. Chattam, M. Nakata, Y. Takanishi, E. Korblova, D. R. Link, R.-F. Shao, W. G. Jang, J. E. Maclennan, O. Mondainn-Monval, V. Boyet, W. Weissflog, G. Pelzl, L.-C. Chien, J. Zasadizinski, J. Watanabe, D. M. Walba, H. Takezoe and N. A. Clark, *Science*, 2003, **301**, 1204.

16 C. H. Legge and G. R. Mitchell, *J. Phys. D, Appl. Phys.*, 1992, **25**, 492.

17 T. A. Krentsel, O. D. Lavrentovich and S. Kumar, *Mol. Cryst. Liq. Cryst.*, 1997, **304**, 463.

18 Y. Lansac, M. A. Glaser, N. A. Clark and O. D. Lavrentovich, *Nature*, 1999, **398**, 54.